Evolution of fractal particles in systems with conserved order parameter

S. V. Kalinin,[1] D. L. Gorbachev,[2] A. Yu. Borisevich,[1] K. V. Tomashevitch,[3] A. A. Vertegel,[3] A. J. Markworth,[4] and Yu. D. Tretyakov[3]

[1]*Department of Materials Science and Engineering, University of Pennsylvania, Philadelphia, Pennsylvania 19104*

[2]*UVD Sakhalinskoi Oblasti, Sakhalin, Russia*

[3]*Department of Chemistry, Moscow State University, 119899 Moscow, Russia*

[4]*Department of Materials Science and Engineering, The Ohio State University, 2041 College Road, Columbus, Ohio 43210*

(Received 24 May 1999)

Computer simulations of the evolution of fractal aggregates in systems with conserved order parameter are described in this work. The aggregates are generated by diffusion-limited aggregation. This model describes such important processes as annealing of dendrite inclusions in solids, healing of cracks in ceramics, temperature-induced transformations in composites, relaxation of rough surfaces, aging of colloid particles, etc. It is shown that the evolution in fractal media differs significantly from that occurring in initially homogeneous systems and leads to different values of the scaling exponent. A relationship between the fractal dimension, mechanism of relaxation, and scaling exponent was also derived.

PACS number(s): 05.70.Np, 05.45.Df, 64.75.+g

INTRODUCTION

Nowadays, the concept of fractal geometry is widely used for the description of spatially inhomogeneous systems [1–3]. Formation of fractal structures is generic for many nonequilibrium processes. The most classic example is formation of fractal clusters during aggregation in solutions and gases. Dendritelike structures can be formed by nonequilibrium electrochemical precipitation, phase decomposition, etc. Cracks and surfaces forming in fracture processes of certain materials also possess fractal structure. Spatial inhomogeneities pertinent to such systems significantly influence their properties and behavior in various physico-chemical processes, such as mass or heat transport. In recent years, certain specific features of diffusion and reaction processes in fractal media have been extensively studied [4–6] under the assumption that the fractal structure of the substrate remains unchanged. However, the excess surface energy of fractal objects gives rise to a number of evolutionary processes leading to significant structural changes. Relevant physical examples include annealing of dendrite inclusions in solids, healing of cracks in ceramics, temperature-induced transformations in composites, relaxation of rough surfaces, aging of colloid particles, etc. In all these cases, the total amount of matter is constant and the evolution is driven by the excess surface or interfacial energy. Surface-tension-driven coarsening of fractal aggregates for different mass transport mechanisms was studied in [7–11]. For evaporation-deposition dynamics, the coarsening process can be well described within the well-known Cahn-Hilliard theory [11,12].

In the present research, the Ostwald-ripening type of evolution of fractal aggregates under conservative conditions is studied. The process is assumed to be limited by volume diffusion. Results obtained by means of computer modeling are compared to the evolution of the homogeneous system. A theoretical model, based on a linear relaxation equation for rough surfaces, is proposed for description of the process.

COMPUTER SIMULATIONS

The fractal aggregates were generated by a diffusion-limited aggregation (DLA) mechanism on a square lattice. The seed was placed in the middle of a 512×512 field. Particles were launched, one at a time, from a reflecting equal-event boundary and performed a random walk until a collision occurred with a growing cluster. Upon collision, the particle either sticks to the cluster, with a new particle being launched from the boundary, or it reflects and continues its random walk. The sticking probabilities P_n to a site with n neighbors were defined as

$$P_n = \min[e^{E(n-4)},1], \tag{1}$$

where E is a constant, so that the probability of sticking to a site with the maximal number of neighbors, $n=4$, is always equal to 1. Larger E values correspond to increasing probability for the particle to stick to a site having a larger number of neighbors, and thus lead to denser clusters. For these simulations, E values were taken to be 0, 0.1,..., 2. The cluster size was chosen to be 3×10^5 particles. The fractal dimension D, as determined by the box-counting method, was 1.72 ± 0.01 for all clusters. However, the lower cutoff of fractality R_a ($R_a\approx2S/P$, where S is the two-dimensional volume of the fractal aggregate, and P is the perimeter) increases with E (Fig. 1).

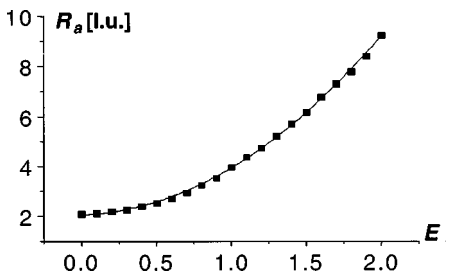

FIG. 1. Lower cutoff of fractality R_a (in lattice units) for DLA clusters grown with different E values.

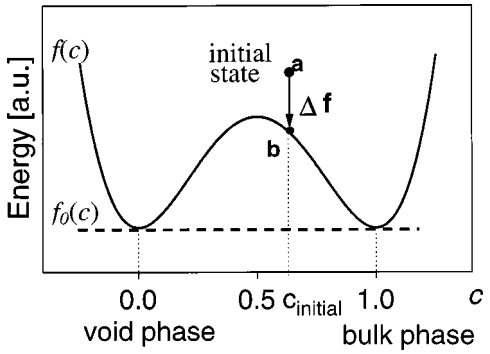

FIG. 2. Free-energy density $f(c)$ as a function of dimensionless concentration.

The temporal evolution of a fractal cluster was described by the evolution equation for systems with conserved order parameter (Fick's second law):

$$\frac{\partial c}{\partial t} = -M\nabla^2 \frac{\delta F}{\delta c}, \tag{2}$$

where c is a dimensionless concentration, $1 \geqslant c \geqslant 0$, and M is the particle mobility [13,14].

The free-energy functional was taken to be of the Landau-Ginzburg form,

$$F = \int_V [f(c) + \tfrac{1}{2} k_c (\nabla c)^2] dV, \tag{3}$$

where k_c is a constant related to the interfacial energy [12]. The free-energy density $f(c)$ was taken as $f(c) = A(c - c^2)^2$ with two symmetric minima corresponding to bulk $(c = 1)$ and void $(c = 0)$ phases (Fig. 2). Thus, the resulting evolution equation was

$$\partial c / \partial t = -M\nabla^2 [k_c \nabla^2 c - 2A(c - 3c^2 + 2c^3)]. \tag{4}$$

Equation (4) was solved by the explicit Euler method on a 512×512 grid with a 0.01 time step. For longer times, the semi-implicit Fourier method [15] was used. Parameters in Eq. (4) were taken as $M = 1$, $k_c = 1$, and $A = 0.25$. A concentration field corresponding to a fractal cluster generated by the modified DLA mechanism was used as the initial condition, $c(\mathbf{r},0)$. Periodic boundary conditions were used. During the evolution, the correlation function of the object, defined as

$$C(\mathbf{r},t) = \langle c(\mathbf{r}+\mathbf{r}',t)\ c(\mathbf{r}',t) \rangle, \tag{5}$$

where the average is taken over the whole system, was calculated. Bulk and surface fractal dimensions of clusters were estimated by means of the box-counting method.

Depending on the ratio between the gyration radius R_g and lower cutoff of fractality R_a of initial clusters, two possible scenarios of evolution were observed: evolution without fragmentation of the initial cluster (Fig. 3) and evolution with fragmentation (Fig. 4).

In the first case, the finer details of the structure of the object are gradually smoothed out, while the larger structural features remain unchanged. The characteristic size of smoothed regions increases with time. However, the overall shape of the aggregate resembles that of the initial cluster.

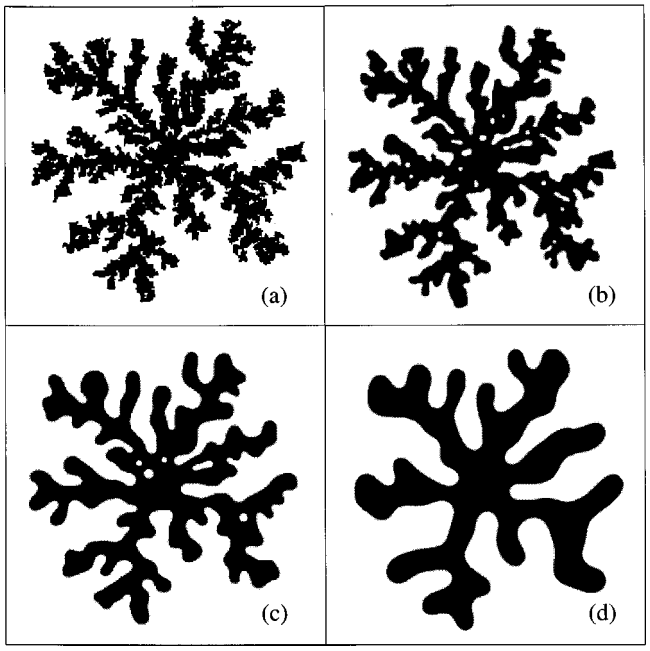

FIG. 3. Evolution of a fractal aggregate $(E = 1.5)$ without fragmentation: (a) initial cluster, (b) $t = 10$ t.u., (c) $t = 100$ t.u., (d) $t = 400$ t.u.

In the second case, the initial cluster rapidly dissociates, forming many small particles [Fig. 4(b)]. Smaller particles dissolve and larger particles grow as in the classical Lifshitz-Slyozov-Wagner model [16–18]. However, due to the inhomogeneous spatial distribution of particles stipulated by the branched structure of the initial aggregate, they have a characteristic elongated form with the larger axis directed parallel

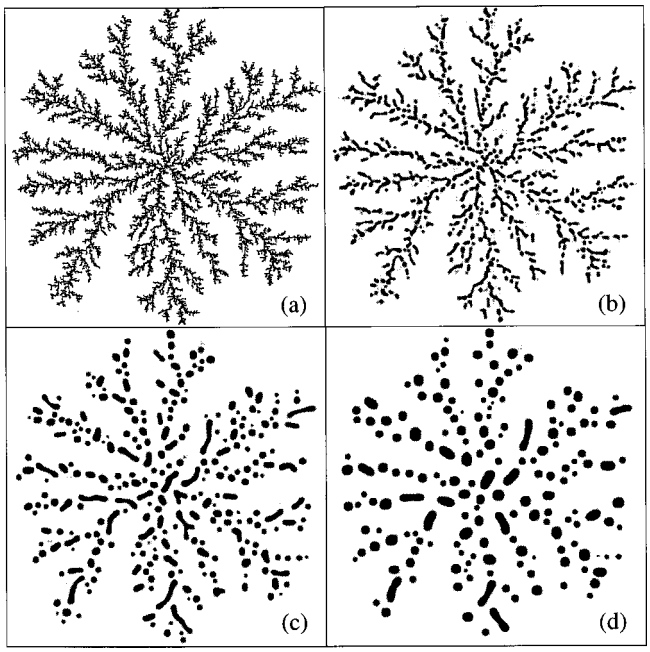

FIG. 4. Evolution of a fractal aggregate $(E = 0)$ with fragmentation: (a) initial cluster, (b) $t = 10$ t.u., (c) $t = 100$ t.u., (d) $t = 400$ t.u.

to the branch of the cluster from which it evolved [Fig. 4(c)]. Subsequent evolution leads to spheroidization of fragments with increased separation between them. However, the spatial distribution of the spherical fragments resembles the structure of the initial cluster [Fig. 4(d)]. Both scenarios will eventually lead to the formation of a single spherical particle, but that would require an extremely long computational time.

Taking into account the diffusion stability of rods in two dimensions, one can assume that the scenario with fragmentation is an artifact of finite lattice size, even though some interesting qualitative patterns were observed. Thus, further theoretical considerations will be limited to the case of evolution without fragmentation.

THEORY

It is well known that during the late stages of the evolution of phase-separating systems described by Eqs. (2) and (3), well-defined domains of bulk ($c=1$) and void ($c=0$) phases form. The corresponding interfacial energy is

$$\sigma=\int_0^1 dc\sqrt{2k_c[f(c)-f_0(c)]}, \tag{6}$$

where $f_0(c)$ is the equilibrium free energy of the mixture, represented by the common tangent line (see Fig. 2).

Since only one domain exists if the evolution occurs without fragmentation, the evolution in this case is equivalent to the surface-tension-driven relaxation of the rough one-dimensional surface of the cluster. The surface can be described by a local height function $h(\mathbf{x},t)$, $\mathbf{x}$ being the coordinate taken along the surface. The mechanism of mass transport in this case is volume diffusion.

The general linearized growth equations for such a process can be expressed as [19]:

$$\frac{\partial h}{\partial t}=-(-\nu\nabla^2)^m h+\eta, \tag{7}$$

where $\nu=M\sigma$. Here, $m=1$ corresponds to growth in the presence of external current (i.e., deposition of material) and $m=2$ corresponds to evolution under conservative conditions. Also, η is the stochastic noise term, assumed to be Gaussian and uncorrelated, i.e., satisfying the condition

$$\langle\eta(\mathbf{x},t)\,\eta(\mathbf{x}',t')\rangle=D_c\delta^d(\mathbf{x}-\mathbf{x}')\,\delta(t-t'), \tag{8}$$

where D_c is a constant $\sim T$ and d is the dimensionality of the embedding space.

Equation (7) can be solved by the Fourier method. Introducing Fourier transforms for $h(\mathbf{x},t)$ and $\eta(\mathbf{x},t)$ as

$$h(x,t)=\int dq\, h_{\mathbf{q}}(t)\exp(i\mathbf{q}\cdot\mathbf{x}) \tag{9}$$

and

$$\eta(x,t)=\int dq\ \eta_{\mathbf{q}}(t)\exp(i\mathbf{q}\cdot\mathbf{x}), \tag{10}$$

Eq. (7) in the Fourier domain can be written as

$$\frac{\partial}{\partial t}h_{\mathbf{q}}=-\nu|\mathbf{q}|^z h_{\mathbf{q}}+\eta_{\mathbf{q}} \tag{11}$$

where $z=2m$. Odd values of z can appear when the relaxation dynamic is nonlocal, e.g., $z=1$ corresponds to diffusion-limited erosion or relaxation through plastic flow, while $z=3$ describes the relaxation through volume diffusion [19], whereas $z=4$ corresponds to evolution under conservative conditions.

The solution for Eq. (11) is

$$h_{\mathbf{q}}(t)=\exp(-\nu|\mathbf{q}|^z t)h_{\mathbf{q}}(0)+\int_0^t d\tau\exp[-\nu|\mathbf{q}|^z \times(t-\tau)]\,\eta_{\mathbf{q}}(\tau), \tag{12}$$

where Fourier transforms of the noise satisfy the following condition:

$$\langle\eta_{\mathbf{q}}(\mathbf{x},t)\,\eta_{\mathbf{q}'}(\mathbf{x}',t')\rangle=D_c L^{-d}\delta_{\mathbf{q}+\mathbf{q}'}\,\delta(t-t'). \tag{13}$$

We assume that the $h_{\mathbf{q}}(0)$ components are not zero, but noise is negligible. Indeed, in our simulations, the noise was solely due to the numerical uncertainties and its amplitude was very small. Thus, Eq. (12) reduces to

$$h_{\mathbf{q}}(t)=\exp(-\nu|\mathbf{q}|^z t)h_{\mathbf{q}}(0). \tag{14}$$

Let us now consider the case of a two-dimensional fractal particle with a one-dimensional surface. In order to estimate the time dependence of the total length L of the surface we write down the following expression for L:

$$L=\int dx\sqrt{1+(h_x')^2}. \tag{15}$$

Assuming small gradients in Eq. (15) and expanding to the first order in $h'(x)$, we obtain

$$L=\int dx\left(1+\frac{(h_x')^2}{2}\right)=L_0+\tfrac{1}{2}\int dx(h_x')^2. \tag{16}$$

From Eq. (9) we obtain the following formula for $h'(x)$:

$$h'(x,t)=i\int dq\, q h_q(t)\exp(iq\cdot x). \tag{17}$$

Substituting Eq. (17) into Eq. (16), we get for the integral

$$\int dx(h_x')^2=-\int\int dq\,dq'qq'h_q(t)h_{q'}(t)\int dx \times\exp[i(q+q')x] \tag{18}$$

or

$$\int dx(h_x')^2=\int dq\,S(q,t), \tag{19}$$

where

$$S(q,t)=h_q(t)h_{-q}(t) \tag{20}$$

is the structure factor at time t.

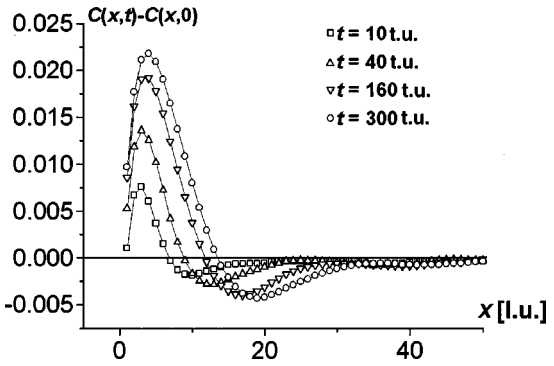

FIG. 5. The effective correlation function $\check{C}(x,t)$ of fractal cluster with $E=2$ for different times of evolution.

Substituting the Fourier components from Eq. (14), we obtain

$$\int dx(h_x')^2 = \int dq\, h_q(0)h_{-q}(0)\exp[-2|q|^z t] = \int S(q,0)\exp[-2|q|^z t] \tag{21}$$

where $S(q,0)$ is the structure factor of the initial surface.

Since, for the fractal aggregate in the region of interest, the structure factor behaves as $S(q,0)\sim q^{2-D}$, we obtain the following equation:

$$\int dx(h_x')^2 = \int dq\, q^{2-D}\exp[-2|q|^z t]. \tag{22}$$

Assuming that the integration is taken from $q=0$ to $q=\infty$ (i.e., the fractal is ideal), integration of Eq. (22) yields

$$\int dx(h_x')^2 = \frac{1}{z}(2\nu t)^{(D-3)/z}\Gamma\left(\frac{3-D}{z}\right). \tag{23}$$

Substituting this expression into Eq. (16) yields

$$L = L_0(1+kt^{(D-3)/z}). \tag{24}$$

For small times it can be approximated as

$$L = L_0 kt^{(D-3)/z}. \tag{25}$$

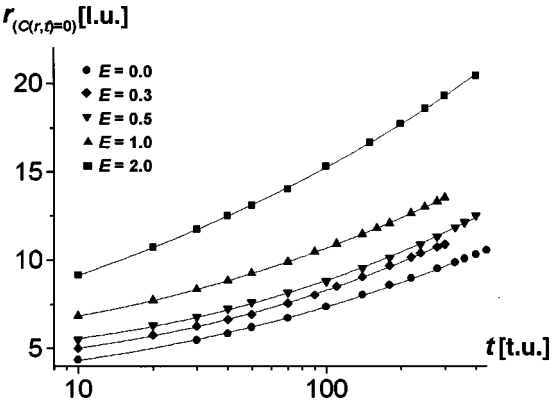

FIG. 6. First zero of effective correlation function (in lattice units) as a function of time for fractal clusters with different E.

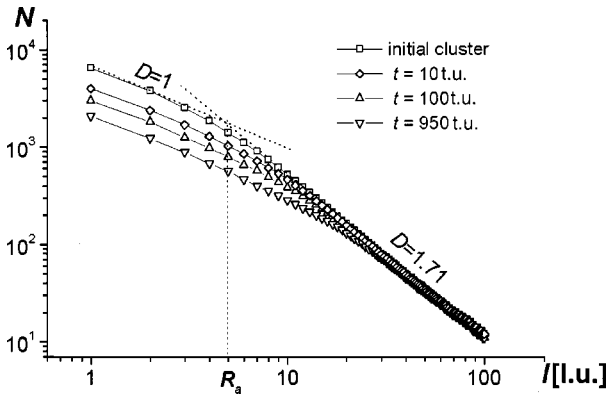

FIG. 7. Box-counting analysis of fractal cluster with $E=2$ for different times of evolution.

On the other hand, for the fractal surface the length is equal,

$$L \sim L_0 R_0^{-D}, \tag{26}$$

where R_0 is the lower cutoff of fractality.

Equating Eqs. (25) and (26) yields the following power law dependence for R_0:

$$R_0 \sim t^{(3-D)/zD} \sim t^{\alpha}. \tag{27}$$

Thus, provided the value of the fractal dimension of the particle and the mechanism of relaxation are known, we can calculate the time dependence of the lower cutoff of fractality. For example, when a typical DLA fractal with $D=1.71$ undergoes relaxation under conservative conditions ($z=4$), the exponent α will be equal to 0.19.

RESULTS AND DISCUSSION

The structural changes that occur during the evolution of fractal aggregates were investigated by the analysis of correlation functions of the resulting structures. It was shown that, for large x, the correlation function $C(x,t)$ for time t is almost the same as that for the initial cluster, $C(x,0)$, in the full agreement with [11]. The effective correlation function of the system, $\check{C}(x,t)=C(x,t)-C(x,0)$, has a characteristic shape (Fig. 5). Due to the increase of the characteristic size of the particles, the value of $C(x,t)$ grows in comparison

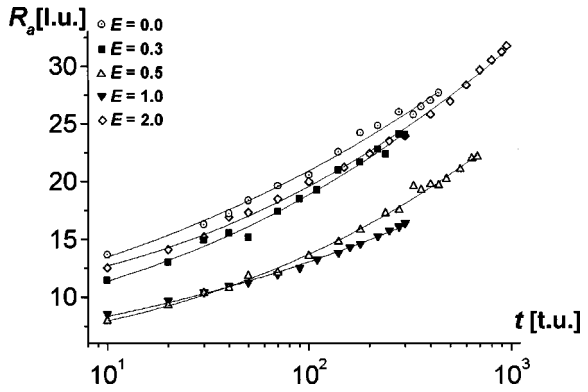

FIG. 8. Lower cutoff of fractality (in lattice units) as a function of time for fractal clusters with different E.

TABLE I. Parameters A, B, and α in Eq. (28) obtained from the analysis of correlation functions.

E	A	B	α
0.0	2.32 ± 0.05	2.2 ± 0.9	0.249 ± 0.003
0.3	2.44 ± 0.07	5.7 ± 1.3	0.262 ± 0.005
0.5	2.73 ± 0.08	7.0 ± 1.4	0.252 ± 0.005
1.0	3.92 ± 0.03	3.2 ± 0.3	0.216 ± 0.001
1.5	4.40 ± 0.05	13.0 ± 1.0	0.205 ± 0.002
2.0	5.73 ± 0.06	-1.0 ± 0.4	0.213 ± 0.002

TABLE II. Parameters A, B, and α in Eq. (28) obtained from the box-counting analysis of the surface.

E	A	B	α
0.0	8.7 ± 0.5	0.0 ± 3.0	0.19 ± 0.01
0.3	6.6 ± 0.6	-1.2 ± 3.6	0.23 ± 0.02
0.5	4.2 ± 0.3	2.0 ± 3.0	0.25 ± 0.01
1.0	4.7 ± 0.2	6.6 ± 1.9	0.22 ± 0.01
1.5	5.0 ± 0.5	32 ± 11	0.21 ± 0.01
2.0	7.3 ± 0.3	3.7 ± 2.7	0.21 ± 0.01

with $C(x,0)$, thus leading to positive values of $\check{C}(x,t)$ for small x. At the same time, for relatively large x the neighborhood is depleted, thus leading to the characteristic minimum of $\check{C}(x,t)$. For large x, $C(x,t)$ does not change compared to $C(x,0)$ and thus $\check{C}(x,t)\approx 0$.

The first zero of $\check{C}(x,t)$, which we denote x_c, roughly corresponds to the mean size of single-phase domains. The temporal dependence of x_c shown on Fig. 6 can be well approximated by the equation

$$x_c = A(t+B)^{\alpha}. \tag{28}$$

where A and B are constants and α is a scaling exponent. The constant B is determined by early-stage evolution of the system [20,21].

Structural changes occurring during evolution were also studied by box-counting analysis of the surface (Fig. 7). The cluster was covered by a square grid with characteristic size l, and the number of squares, N, containing at least one point belonging to the cluster surface was plotted as a function of l in log-log coordinates. For relatively small l, the slope of the corresponding curve is 1 (the surface is one dimensional), whereas for larger l, the slope is equal to the fractal dimension of the object, $D=1.71$. The intersection of these two linear segments defines the characteristic length R_a, also proportional to the characteristic length scale on which the fractal structure is destroyed (Fig. 8).

Results of the correlation function analysis, x_c vs t, for clusters with different E, are shown in Table I, and for the box-counting analysis, R_a vs t, in Table II. For evolution without fragmentation, values obtained for the scaling exponents α agree well. The values lie in the range 0.21 ± 0.01 for all structures, thus exhibiting good agreement with theory. It should be noted that values obtained for B are relatively small (B is much less than the characteristic time of evolution), i.e., the characteristic size of the single-phase domain grows by a power law, $L(t)\sim t^{\alpha}$.

For evolution with fragmentation, values obtained for the scaling exponents α are larger than in the first case. Numerical values of scaling exponents, determined from correlation function analysis and box-counting analysis, are significantly different, probably due to problems with the box-counting analysis for a system having relatively small isolated particles. Interestingly, for later stages of evolution, a transition to $\alpha=\frac{1}{3}$ takes place when the initial fractal structure of the cluster is completely destroyed, and evolution proceeds as in the initially homogeneous system.

CONCLUSIONS

The evolutionary path of the system was shown to depend on the geometry of the initial particle as described by the lower cutoff of fractality R_a and gyration radius R_g and the value of the fractal dimension D. The following main features of the evolution were determined.

During the evolution, the fractal structure is destroyed on small length scales; however, on the larger length scales, it is generally conserved.

The value of the scaling exponent for the evolution of a fractal particle without fragmentation, $\alpha=0.21\pm0.01$, is substantially different from that in the homogeneous case, $\alpha=0.33\pm0.01$. For evolution with fragmentation, the apparent value of the scaling exponent increases with R_a/R_g. For the late stages of evolution α presumably reaches the value of $\frac{1}{3}$.

The theory developed above has been proven valid in this particular case. It can possibly be applied for prediction of behavior of other inhomogeneous systems in diffusion-driven evolutionary processes, thus providing some guidelines for further modeling and experimental studies.

ACKNOWLEDGMENTS

This work was partially supported by the Russian Foundation for Basic Research Grant No. 96-03-33122a, Universities of Russia Program Grant No. 98-06-14-5650, NATO Linkage Grant No. 970608, and International Soros Educational Program Grant Nos. a98-1724, s98-1716, and s98-1348.

[1] B. B. Mandelbort, *The Fractal Geometry of Nature* (W. H. Freeman, New York, 1983).

[2] *Fractals and Disordered Systems*, edited by A. Bunde and S. Havlin (Springer-Verlag, New York, 1991).

[3] *The Fractal Approach to Heterogeneous Chemistry*, edited by D. Avnir (Wiley, New York, 1989).

[4] J. S. Havlin and D. Ben-Avraham, Adv. Phys. **36**, 695 (1987).

[5] M. Sahimi, Chem. Phys. **64**, 21 (1996).

[6] M. Giona, W. A. Schwalm, M. K. Schwalm, and A. Adrover, Chem. Eng. Sci. **51**, 4717 (1996); **51**, 4731 (1996); **51**, 5065 (1996).
[7] R. Sempere *et al.*, Phys. Rev. Lett. **71**, 3307 (1993).
[8] T. Irisawa, M. Uwaha, and Y. Saito, Europhys. Lett. **30**, 139 (1995).
[9] N. Olivi-Tran, R. Thouy, and R. Jullien, J. Phys. I **6**, 557 (1996).
[10] R. Thouy, N. Olivi-Tran, and R. Jullien, Phys. Rev. B **56**, 5321 (1997).
[11] M. Conti, B. Meerson, and P. V. Sasorov, Phys. Rev. Lett. **80**, 4693 (1998).
[12] J. W. Cahn and J. E. Hilliard, J. Chem. Phys. **28**, 258 (1958).
[13] Y. Wang, L. Q. Chen, and A. G. Khachaturyan, in *Computer Simulation in Materials Science: Nano/Meso/Macroscopic Space and Time Scales*, edited by H. O. Kirchner, L. P. Kubin, and V. Pontikis (Kluwer Academic, Boston, 1996), p. 325.
[14] A. J. Bray, Adv. Phys. **43**, 357 (1994).
[15] L. Q. Chen and J. Shen, Comput. Phys. Commun. **108**, 147 (1998).
[16] I. M. Lifshitz and V. V. Slyozov, Zh. Eksp. Teor. Fiz., **35**, 479 (1959) (in Russian) [Sov. Phys. JETP **35**, 331 (1959)].
[17] I. M. Lifshitz and V. V. Slyozov, J. Phys. Chem. Solids **19**, 35 (1961).
[18] C. Wagner, Z. Elektrochem. **65**, 581 (1961).
[19] J. Krug, Adv. Phys. **46**, 139 (1997).
[20] G. Ramirez-Santiago and A. E. Gonzalez, Physica A **236**, 75 (1997).
[21] J. D. Gunton, M. San Miguel, and P. S. Sahni, in *Phase Transitions*, edited by C. Domb and J. E. Lebowitz (Academic Press, London, 1983), p. 267.